



## Frequency-selective non-linear blending for the computed tomography diagnosis of acute gangrenous cholecystitis: Pilot retrospective evaluation

R. Schwarz<sup>a,\*</sup>, N.M. Bongers<sup>a</sup>, C. Hinterleitner<sup>b,1</sup>, H. Ditt<sup>c</sup>, K. Nikolaou<sup>a</sup>, J. Fritz<sup>d</sup>, H. Bösmüller<sup>e,1</sup>, M. Horger<sup>a,1</sup>

<sup>a</sup> Department of Diagnostic and Interventional Radiology, Eberhard-Karls-University, Hoppe-Seyley-Str. 3, 72076 Tuebingen, Germany

<sup>b</sup> Department of Internal Medicine II, Eberhard-Karls-University, Otfried-Müller-Str. 8, 72076 Tuebingen, Germany

<sup>c</sup> Siemens Healthcare GmbH, Diagnostic Imaging, Siemensstr. 1, D-91301 Forchheim, Germany

<sup>d</sup> Johns Hopkins University School of Medicine Department of Radiology and Radiological Science, 601 N. Caroline Street, JHOC 3142, Baltimore, Maryland, 21287, United States

<sup>e</sup> Institute of Pathology, Eberhard-Karls-University, Liebermeisterstr. 9, 72076 Tuebingen, Germany

### ARTICLE INFO

#### Keywords:

Acute cholecystitis  
Gangrenous cholecystitis  
Post processing CT imaging  
Frequency selective non linear blending  
Emergency  
CT

### ABSTRACT

**Purpose:** To compare the diagnostic performance of frequency-selective non-linear blending and conventional linear blending contrast-enhanced CT for the diagnosis of acute (AC) and gangrenous (GC) cholecystitis.

**Materials and methods:** Following local ethics committee approval for retrospective data analysis, a database search derived 39 patients (26 men, mean age  $67.8 \pm 14.6$  years) with clinical signs of acute cholecystitis, contrast enhanced CT (CECT) evaluation, cholecystectomy, and pathological examination of the resected specimen. The interval between CECT and surgery was  $4.7 \pm 4.1$  days. Pathological gross examination was used to categorize the cases into AC and GC. Subsequently, two radiologists categorized the CECT studies in a blinded and independent fashion into AC and GC, during two different reading sessions using linear blending and frequency-selective non-linear blending CECT.

**Results:** Histologic analysis diagnosed 31/39 (79.4%) cases of GC and 8/39 (20.6%) cases of AC. Image interpretation of linear blending CECT resulted in classification of 7/39 (17.9%) patients as GC and 32/39 (82.1%) as AC, whereas image interpretation of frequency-selective non-linear blending CECT resulted in classification of 29/39 (74.3%) patients as GC and 10/39 (25.7%) as AC. Sensitivity/specificity/PPV/NPV for detection of GC were 22.6%/100%/100%/25% with linear blending CECT and 80.6%/50%/86.2%/40% with frequency-selective non-linear blending CECT, respectively. Based on the histopathologic diagnosis frequency-selective non-linear blending had a significant improvement ( $p > 0.0001$ ) in the diagnostic accuracy of gangrenous cholecystitis compared with linear blending.

**Conclusion:** Frequency-selective non-linear blending post-processing increases the diagnostic accuracy of gangrenous cholecystitis owing to improved visualization of absence of focal enhancement and mural ulcerations.

### 1. Introduction

Acute cholecystitis (AC) is a frequent cause of severe abdominal pain that often requires surgical treatment [1–4]. While AC can be diagnosed based on typical symptoms and several inflammatory markers, cross-sectional imaging is often used to confirm the diagnosis and diagnose potential mimics. Ultrasound and computed tomography (CT) have been used most frequently, whereas magnetic resonance imaging has not shown relevant advantages in diagnosis [1,4,5].

Different imaging findings for the diagnosis of acute gangrenous cholecystitis, including decreased or absent mural enhancement, intramural or intraluminal gas, irregular wall thickening, perforation, pericholecystic abscess and pericholecystic stranding have been described [1,6–10] whereas for acute non-gangrenous cholecystitis gallbladder wall thickening with edema pattern and layering, sloughing of the inner layer of the gallbladder wall, hyperattenuation of the gallbladder fossa, pericholecystic fluid, gall bladder distension and gallstones are usually expected [6,9,11,12]. The findings mural striation

\* Corresponding author.

E-mail address: [ricarda.schwarz@med.uni-tuebingen.de](mailto:ricarda.schwarz@med.uni-tuebingen.de) (R. Schwarz).

<sup>1</sup> These authors share equal contribution.

and intraluminal membranes, were discussed controversially [1,2]. Using histology as a standard of reference, findings such as thinning and erosive irregularities of the gallbladder wall have been found to be more often present in gangrenous cholecystitis [1,6,7,13]; however, great overlap exists between both entities and absent wall enhancement, ulcerations, and perforation are the most reliable findings of transmural necrosis [1,8,13].

An accurate imaging diagnosis is important for treatment decisions such as surgical versus systemic antibiotic treatment, and for the surgical approach, such as laparoscopic versus open cholecystectomy. Systemic antibiotic therapy and in select cases percutaneous cholecystostomy may be suitable alternatives to cholecystectomy in patients with high perioperative risk factors, but require the exclusion of gangrenous cholecystitis [3,7,11,14].

Improved tissue contrast can improve the detectability of gangrenous and non-gangrenous acute cholecystitis through improved visibility of signs of transmural necrosis of the gall bladder wall. Increasing the tube current, as well as volume and concentration of iodine-based contrast agents may be beneficial but come with concerns of increasing radiation dose and potential for impairment of renal function. The possibility of low-kilovolt acquisition to increase iodine attenuation closer to the k-edge is not available on all CT-scanners, whereas the use of low-keV monoenergetic extrapolation is limited to dual-energy CT acquisitions. Contrary to linear blending, which affects the entire dynamic contrast range, frequency-selective non-linear blending can be applied to a select range of Hounsfield units, e.g. in the low-keV range to improve the visibility of possibly undetectable small differences in tissue contrast [15–18]. Frequency-selective non-linear blending is independent of the acquisition technique and can be applied to single and dual energy CT data.

Therefore, the purpose of our study was to compare the diagnostic performance of the novel technique called frequency-selective non-linear blending with that of conventional linear blending applied on contrast-enhanced CECT image data for differentiation between acute non-gangrenous vs. gangrenous cholecystitis.

## 2. Material and methods

### 2.1. Patient selection

This retrospective data evaluation was approved by the local institutional ethics committee of the Eberhard-Karls-University Tuebingen, Germany and registered under the number 791/2017BO2. The Declaration of Helsinki protocols were followed. The informed consent requirement was waived. A database research between January 2010 and October 2017 derived 350 pathological examinations of gall bladder specimens. Of them, 311 were excluded due to diagnoses of chronic cholecystitis and neoplastic disease, small gallbladder specimens in the database that was insufficient for reexaminations, lack of CECT during presurgical work-up.

The remaining 39 patients were included in the final evaluation (mean age  $67.8 \pm 14.6$  years; range 33–92 years; 33% women). The length of time between CECT and surgery was  $4.7 \pm 4.1$  days. All included patients presented with clinical signs of acute cholecystitis and underwent single energy CECT evaluation, were treated with cholecystectomy, and had a pathological examination of the resected specimen.

### 2.2. Histologic diagnosis

Following cholecystectomy and formalin fixation, representative cross sections of the most abnormal area of the gall bladder and the resection margin of the cystic duct were taken from each specimen. The histologic slides were retrieved from the appropriate paraffin embedded material and stained with hematoxylin and eosin. Necrosis was defined as transmural wall devitalization, whereas wall defects of the inner

layer were diagnosed as ulcers. Gangrenous cholecystitis was diagnosed if at least one of following three criteria were met: Transmural necrosis, laminar ulcers, and gallbladder wall perforation. Acute cholecystitis was diagnosed in the presence of wall thickening secondary to edema, infiltration with inflammatory cells and granulation tissue, and lack of tissue necrosis [19,20]. One pathologist (H.B.) with 20 years of experience re-evaluated every case included in our study.

### 2.3. Computed tomography technique

CT studies were performed with patients in the supine position using 128-256-slice MDCT scanners (SOMATOM Definition AS+, Flash or Force, Siemens Healthcare, Forchheim, Germany). All patients received 100 ml iodinated contrast agent Imeron 400 (Bracco, Imaging Deutschland GmbH), which was given intravenously at a rate of 2 mL/s followed by a 30 ml saline chaser. Contrast medium was administered by using a dual-head pump injector (Stellant, Medtron, Saarbruecken, Germany). Post-contrast images were obtained in the portal-venous phase following a delay time of 70–80 seconds in all patients using 100 kV and tube current dose modulation. Images were reconstructed at 1 mm and 3 mm using a soft tissue kernel and a matrix of  $512 \times 512$ . For interpretation of linear blending and frequency-selective non-linear blending CECT images, axial reformations of 3 mm slice thickness were used, which parallels our clinical practice. The length of time of image data pre- and post-processing was approximately 3.5 min, including 120 s for image data transfer to the workstation where the prototype software was installed; 60 s for loading of images with the prototype software, and 30 s for adjusting the viewing parameters (see below).

### 2.4. Conventional CECT evaluation

Two radiologists (M.H. and R.S.) with 27 and 2 years of experience in abdominal imaging interpreted the conventional linear blending CECT images with use of a questionnaire for the presence or absence of ulcers (focal missing enhancement of the inner layer), focal/patchy pattern of necrosis (patchy/focal enhancement of all layers), diffuse necrosis of all layers (visually below the liver parenchyma), perforation (discontinuous gall bladder wall with fluid in the gall bladder fossa), striation, pericholecystic abscess, enhancement of the adjacent liver parenchyma, sludge/sedimentation, cholelithiasis, pericholecystic lymphadenopathy, inflammatory reaction of the duodenum or the right colic flexure. Intramural gas was not included in the questionnaire, but not present in our cohort. The definition of these criteria was in line with that of previous reports dealing with this issue [1,6,9,10,13]. Prior to image interpretations, the two radiologists were provided with the definitions and image examples of the imaging signs of the questionnaire and underwent basic training using 10 patients with acute, chronic and gangrenous cholecystitis that were not included in this study. The interpretation of the study cases was performed following separation and randomization of corresponding linear blending and frequency-selective non-linear blending CECT datasets. The two radiologists performed the imaging analysis using the same criteria and questionnaires following a three weeks interval to limit recall bias and the intraobserver agreement was calculated. For statistical evaluation the first interpretation of the more experienced radiologist was used.

### 2.5. Image analysis using frequency-selective non-linear blending

For the frequency-selective non-linear blending reading session, all CT images – performed in daily routine with a soft tissue kernel B30 and filtered back projection reconstruction with conventional linear weighting of frequencies – were transferred to an external offline workstation with a frequency-selective non-linear blending prototype software (Siemens Healthineers) [15–18]. The algorithm enabling non-linear blending of CT images first divided image information into low and high frequencies, whereas high frequencies represented the main

part of image noise and low frequencies included contrast information. Second, a non-linear scaling function was propagated to low frequencies to highlight pixel intensities in a defined subset of the entire dynamic range (delta). Image intensity could be influenced by adapting the slope and delta of the subset. During post-processing, the parameters such as centre, delta, and slope were defined manually to pre-select the interesting sector of Hounsfield unit (HU) values. Centre described the centre value, and delta described the range of influenced HU values. Selecting the slope between 0 and 5 adapted the relative contrast enhancement (0, the image will remain unaffected; 5, maximum contrast enhancement). The two readers first underwent a training phase which focussed on optimization of frequency-selective non-linear blending settings using CECT-image data of forty patients with acute cholecystitis and such without gallbladder pathology who were not included in the study. The final frequency-selective non-linear blending settings were set at an averaged centre of 30 HU, an averaged delta of 5 HU and at a slope of 5. No image blending could be performed above upper and below lower thresholds (t1 and t2), which were set at -20 and 100 HU respectively.

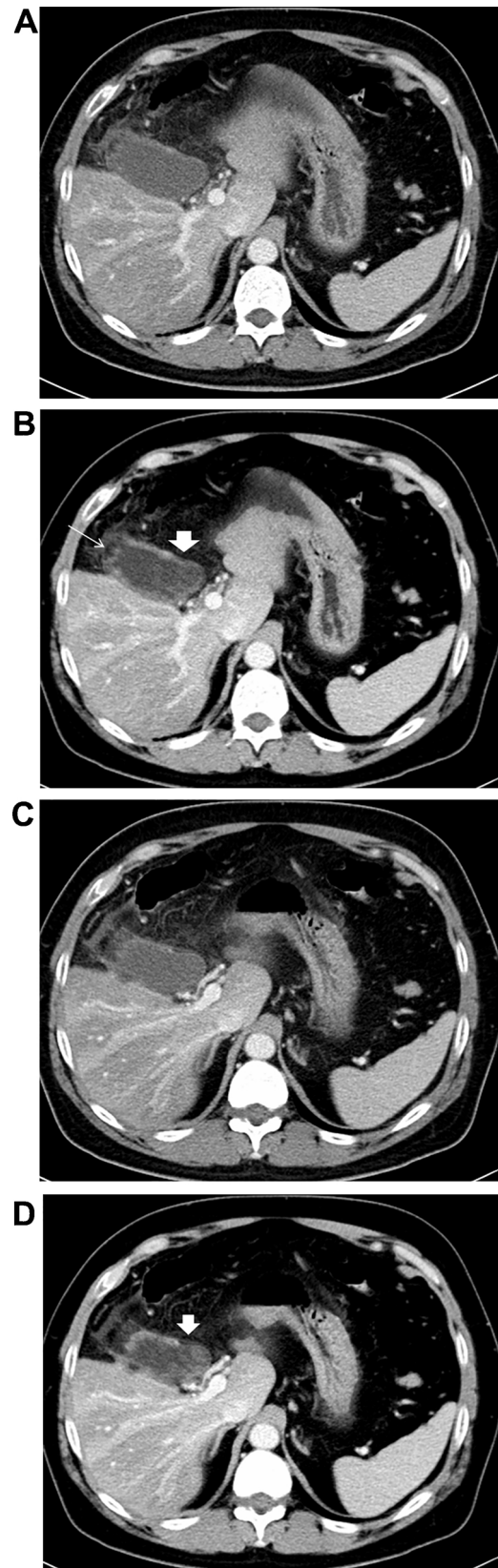
### 2.6. Statistical analysis

Statistical analyses were computed using SigmaStat, Version 21 (SPSS). Descriptive statistics were used to summarize demographic and clinical characteristics of the study population. For comparing the diagnostic accuracy of frequency-selective non-linear blending and linear blending based on the histological diagnosis, we calculated the sensitivity, specificity, positive predictive value (PPV), negative predictive value (NPV) as well as corresponding binomial 95% confidence intervals (CIs); p values were determined using McNemar's test. Fisher's exact test was used to compare the radiologic and histopathologic findings in both frequency-selective non-linear blending and linear blending. The correlation between radiologic and histopathologic finding was investigated using phi coefficient. A phi coefficient < 0.19 was considered no or negligible correlation, < 0.29 a weak positive correlation, < 0.39 a moderate positive, > 0.40 strong positive correlation. All statistical tests were done for every single image finding and also for the combination of ulcer + focal (patchy) pattern of necrosis + diffuse necrosis of all layers + perforation. Combination means that we counted all patients who had at least one of these findings because every imaging criterium alone would be interpreted as gangrenous cholecystitis but not all criteria have to be fulfilled. All statistical tests were considered significant when  $p < 0.05$  (\* < 0.05, \*\* < 0.01; \*\*\* < 0.001). Interobserver and intraobserver agreements were calculated for each imaging finding using the Cohen's kappa. The average was calculated for linear blending and frequency-selective linear-blending. A kappa of < 0.79 was considered as moderate agreement, < 0.90 as strong agreement and > 0.90 as perfect agreement.

### 3. Results

On histological examination there were 16/39 (41%) ulcers, 3/39 (7.6%) erosions and 21/39 (53.8%) transmural necrosis. Hemorrhage was present in 24/39 (61.5%) specimens and scarring was present in 8/39 (20.5%) specimen. Thirty-one (79.4%) specimens were classified as gangrenous cholecystitis, whereas eight (20.5%) specimens were classified as acute cholecystitis.

Using CT images with linear blending, readers diagnosed absent gallbladder wall enhancement in 1 of 39 (2.5%) patients, focal absence of enhancement in 4/39 (10.2%) patients, ulcers in 2/39 (5.1%) patients, and perforation in 7/39 (17.9%) patients, equating to 7/39 (17.9%) diagnoses of gangrenous cholecystitis and 32/39 (82.1%) diagnoses of acute cholecystitis. There was no gallbladder gas. The interobserver and intraobserver agreement for interpretation of linear blending -based image reading was perfect ( $k = 0.93$  and  $k = 0.96$ ,



(caption on next page)

respectively). Twenty-four of 31 (61.5%) of the pathologically diagnosed gangrenous cholecystitis were missed with linear blending, whereas all cases of acute cholecystitis were diagnosed correctly (Figs. 1a–d, 2a–b, 3a–b and 4a–b). Sensitivity/specificity/PPV/NPV for



**Fig. 1.** a–d: 61-year-old male patient referred to CECT for elucidation of acute colicky right abdominal pain. On Fig. 1a linear blending (soft tissue windowing; W 300; C 40) was used showing ill-defined thickened gallbladder wall and pericholecystic fluid. Wall enhancement couldn't be sufficiently assessed on this image. Fig. 1b reveals multifocal absence or markedly reduced gallbladder wall enhancement (arrowhead) compatible with gangrenous cholecystitis. Note disruption of the gallbladder wall in the fundus region with perforation (arrow). Three slices distal from Fig. 1a- and b, linear blending (c) and frequency-selective non-linear blending (d) show again great differences in the assessment of the gallbladder wall in terms of confines and presence/absence of enhancement. Surgery and subsequent histologic examination confirmed multifocal gallbladder wall necrosis.

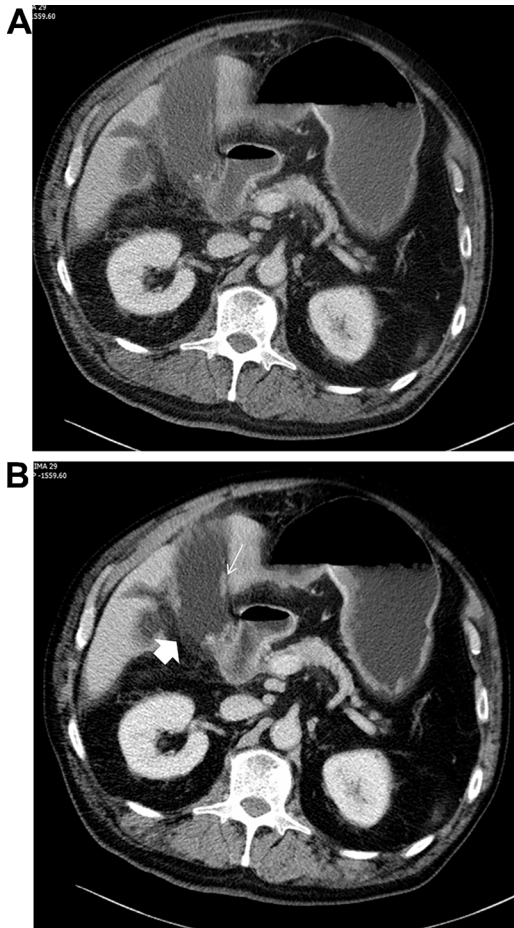


**Fig. 2.** a–b: 79-year-old male patient presenting with acute colicky pains in the upper right abdominal quadrant and referred to CECT for diagnosis. Fig. 2a (linear blending -soft tissue windowing; W 350; C 50) shows ill-defined thickened gallbladder wall as well as pericholecystic fluid. Wall enhancement was discontinuous suggesting ischemia. Note improved delineation of the gallbladder wall on Fig. 2b with multiple areas of necrosis (arrowhead) and skip areas with persistent vascularization (arrow) compatible with gangrenous cholecystitis. At surgery and subsequent histologic examination multifocal gallbladder wall necrosis with skip areas was confirmed. There was also focal hemorrhage in the necrotic tissue at histologic examination.

the combinational findings in linear blending was 22.6%/100%/100%/25%, respectively, phi coefficient 0.24. The single criterium focal/patchy enhancement had the biggest impact on this correlation (phi coefficient 0.17).

Using frequency-selective non-linear blending, readers diagnosed absent gallbladder wall enhancement in 1 of 39 (2.5%) patients, focal absence of enhancement in 24/39 (61.5%) patients, ulcers in 17/39 (43.5%) patients, and perforation in 8/39 (20.5%) patients, equating to 29/39 (74.4%) diagnoses of gangrenous cholecystitis and 10/39

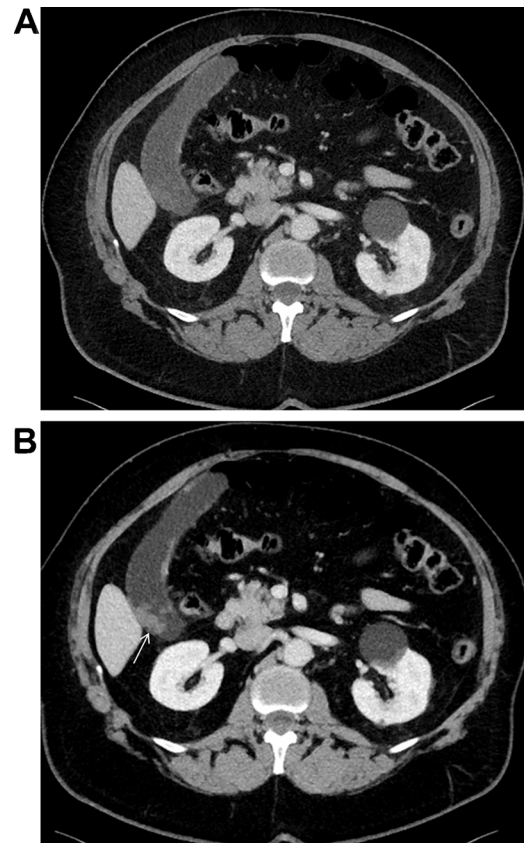


**Fig. 3.** a–b: 65-year-old male patient referred to CECT for acute cholecystitis. On Fig. 3a linear blending (soft tissue windowing; W 350; C 50) shows gallbladder wall thinning, but no clear mucosal enhancement. Fig. 3b (frequency-selective non-linear blending) shows discontinuation of gallbladder wall enhancement with almost entire necrosis compatible with gangrenous cholecystitis. There is also some sludge within the gallbladder (arrow). Surgery and subsequent histologic examination confirmed extensive GB-wall necrosis and hemorrhage.

(25,6%) diagnoses of acute cholecystitis. The interobserver and intraobserver agreement for interpretation of frequency-selective non-linear blending CECT was perfect ( $k = 0.94$  and  $k = 0.95$ , respectively). Of the histologically diagnosed gangrenous cholecystitides, 6/31 (19.3%) were not detected with frequency-selective non-linear blending (false-negative). Four cases with pathologically proven acute cholecystitis were erroneously categorized as gangrenous cholecystitis (false-positive) (Table 1). Sensitivity/specificity/PPV/NPV for the combination of findings in frequency-selective non-linear blending was 80.6%/50%/86.2%/40%, respectively, phi coefficient 0.29. The single criterion focal (patchy) enhancement had the biggest impact on this correlation (phi coefficient 0.25).

Frequency-selective non-linear blending increases the diagnostic accuracy (sensitivity) of gangrenous cholecystitis significantly. The combinational findings (ulcus + focal[patchy] pattern of necrosis + diffuse necrosis of all layers + perforation) were superior (sensitivity in frequency-selective non-linear blending 81%, linear blending 23%,  $p < 0.001$ ) than the single criterium focal/patchy pattern of necrosis (sensitivity in frequency-selective non-linear blending 68%, linear blending 13%,  $p < 0.001$ ). None of the other single criteria had a good correlation with the histopathologic diagnosis (phi coefficient  $< 0.19$ ). In three patients, there was focal absence of gallbladder wall enhancement with frequency-selective non-linear blending, but there was no correlation with pathology. Two of these patients had deep ulcers of the gallbladder wall but no transmural necrosis at the time of histologic diagnosis. One patient had a markedly

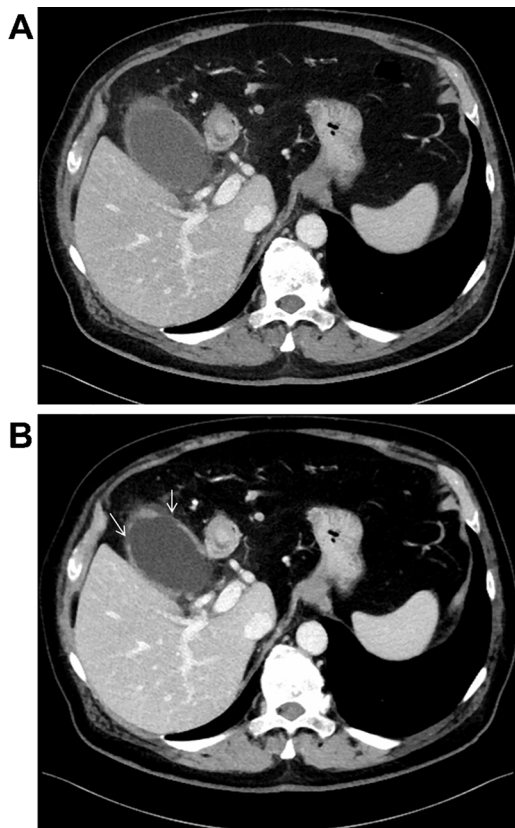


**Fig. 4.** a–b: 78-year-old male patient referred to CECT for acute upper abdominal pain suspected of gastritis. **Fig. 4a** (linear blending-soft tissue window; W 350; C 50) shows slightly thickened GB-wall with minimal enhancement suggesting ischemia (necrosis) and partial wall thinning suggesting large ulcers whereas frequency-selective non-linear blending (**Fig. 4b**) obviously delineates transmural ischemia (arrows). Surgery and subsequent histologic examination confirmed extensive gallbladder wall necrosis and ulcers.

thickened gallbladder wall due to edema which was falsely classified as necrosis (false positive) with frequency-selective non-linear blending CECT.

In total we classified cholecystitis as gangrenous in 7 patients using linear blending and in 27 patients based on results of frequency-selective non-linear blending. Recognition of gangrenous cholecystitis reached significance only for frequency-selective non-linear blending. Using linear blending 70% of gangrenous cholecystitis were missed. Sensitivity/specificity/PPV/NPV for linear blending was 22.6%/100%/100%/25% and for frequency-selective non-linear blending was 80.6%/50%/86.2%/40%, respectively. Therefore, the sensitivity in frequency-selective non-linear blending was 58% higher than in linear blending ( $p < 0.001$ ) using the McNemar's test. Using only the focal absence of wall enhancement as a diagnostic criterion for gangrenous cholecystitis resulted in 21/31 (67.7%) sensitivity, whereas the combined use of all criteria (wall enhancement, ulcers and perforation) yielded a sensitivity of 80.6% (25/31).

#### 4. Discussion

We evaluated the ability of computed tomography to differentiate between acute non-gangrenous and gangrenous cholecystitis using conventional linear blending and frequency-selective non-linear blending post-processing with pathological examination as the standard of reference. Our results indicate that frequency-selective non-linear blending post-processing increases the diagnostic performance of CT for the diagnosis of gangrenous cholecystitis.

Gangrenous cholecystitis is characterized by gallbladder wall

ischemia resulting in absent wall enhancement that can be distributed either diffusely or focally. [11] Non-transmural ischemia leads to formation of ulcers whereas transmural ischemia results in gallbladder wall perforation with pericholecystic abscess [21]. According to our results discrimination between these two types of acute cholecystitis can be significantly improved using frequency-selective non-linear blending.

Hence, frequency-selective non-linear blending showed a 58% higher sensitivity for detection of gangrenous cholecystitis over conventional linear blending, whereas the specificity and the positive predictive value were slightly lower. Notably, the number of detected gallbladder wall ulcers was more than eight times higher with frequency-selective non-linear blending compared to conventional linear blending indicating markedly improved delineation of the gallbladder wall. The gallbladder wall is otherwise frequently difficult to assess in acute cholecystitis due to submucosal edema and also to slightly decreased mucosal enhancement secondary to wall thickening and compression. Pericholecystic fluid is frequent in acute cholecystitis, but it can also be a sign of gallbladder wall perforation. In order to make this differentiation, adequate depiction of the gallbladder wall is essential. This presumably explains why even a case of gallbladder perforation was missed by conventional nonlinear blended images. As only contrast-enhanced CT images were used, the influence of mural hemorrhage on accurate detection of necrosis must be questioned. In this report, we did not focus on the ancillary findings suggesting the diagnosis of acute cholecystitis like wall thickening, intraluminal membranes, mural stratification, pericholecystic fat stranding and free fluid accumulation in the gallbladder fossa that were present in most of the patients because they do not reliably allow for differentiation between acute cholecystitis and gangrenous cholecystitis. Three imaging findings (absence of gallbladder-wall enhancement, ulcers and perforation) have been strongly associated with gangrenous cholecystitis in previous reports [6]. However, the recognition of discontinuous gallbladder-wall enhancement can be severely hampered in CECT using only linear blending due to an inadequate mucosal enhancement as seen in our results [6]. Singh et al. found a sensitivity of only 30.3% for prediction of gangrenous cholecystitis based on the presence of irregular mucosal enhancement. Fuks et al. found a sensitivity of 73% for detection of gangrenous cholecystitis based on the absence of gallbladder-wall enhancement and suggested the use of this information for the purpose of conversion from laparoscopic to open cholecystectomy [8]. In a report by Chang et al., decreased wall enhancement accompanied by marked distension of the gallbladder was found highly significant for gangrenous cholecystitis [1]. In this report, mural enhancement alone was difficult to assess in 30% of the patients. Hence, the accurate detection of wall enhancement seems to be the key to a more reliable classification of acute cholecystitis implying its therapeutic consequences. In frequency-selective non-linear blending the soft tissue contrast of the gall bladder wall can be adjusted in order to highlight focal areas that are either hyper- or hypo-attenuated by increasing or decreasing the lesions own intensities (HU) or that of the background (e.g. liver parenchyma). With this improvement it is much easier to detect focal unenhanced areas which are suspicious for GC. Some other imaging techniques like MRI and contrast-enhanced ultrasound (CEUS) have been tested with more or less success, but their routine use is limited by their conditioned availability in the emergency setting, higher costs or by being strongly operator-dependent and in the first line by limitations related to the cholecystitis itself (e.g. gas in the wall and bile stones hamper visualization of the gallbladder-wall; acute abdominal pain or incipient biliary peritonitis and paralytic ileus impair adequate ultrasound examination [5,22,23]).

Frequency-selective non-linear blending seems to be able to help overcoming these limitations by enabling an increase in tissue contrast for a preselected range of Hounsfield units. Frequency-selective non-linear blending is a post-processing technique affecting only a pre-defined (e.g. between  $I_1$  [-20 HU] and  $I_2$  [100 HU]) range of Hounsfield

**Table 1**  
Independent readings of cholecystitis cases.

	Reader I		Reader II		Reader I		Reader II	
	Total number of findings in all 39 patients	Findings in pathological proven gangrenous cholecystitis (n = 31)	Total number of findings in all 39 patients	Findings in pathological proven gangrenous cholecystitis (n = 31)	Total number of findings in all 39 patients	Findings in pathological proven gangrenous cholecystitis (n = 31)	Total number of findings in all 39 patients	Findings in pathological proven gangrenous cholecystitis (n = 31)
Gallbladder wall								
Ulcer: Focal lack of enhancement of the inner layer	2	2	3	3	17	14	13	10
Focal/patchy pattern of necrosis	4	4	4	4	24	21	21	19
Diffuse necrosis of all layers (visually below that of the liver parenchyma)	1	1	5	4	1	1	3	2
Perforation: Discontinuous wall + fluid in the gall bladder fossa	7	7	5	5	8	8	8	8
Striation of the gallbladder wall	17	14	17	14	29	26	26	21
Pericholecystic abscess	6	5	6	5	6	5	6	5
Enhancement of the adjacent liver parenchyma	3	1	3	1	5	4	4	3
Sludge/Sedimentation	5	4	4	2	19	18	18	17
Cholecystolithiasis	18	15	18	15	21	16	21	16
Cholecholelithiasis	2	1	2	1	2	1	2	1
Pericholecystic lymphadenopathy	4	4	4	4	8	7	7	6
Duodenal reaction (wall thickening, fat stranding)	6	6	4	4	10	9	10	10
right colic flexure reaction (wall thickening, fat stranding)	3	2	3	2	5	3	4	2



unit values generating images with up to 300% improved tissue contrast [18]. The suitable parameter settings we established for diagnosing GC and AC with this application (centre of 30 HU, delta of 5 HU at a slope of 5) significantly differed from previous clinical applications focusing on other pathologies [15–17,24]. The five adjustable parameter settings we are proposing in this report proved generally adequate in our cohort. This beneficial effect is resulting from increased attenuation of iodine which instead is dependent on energy and knowingly enhances at lower kV levels because of the predominance of the photoelectric effect closer to the K-edge of iodine [25,26]. Similar attempts have been made so far by using virtual monoenergetic low-kV [18]. These authors demonstrated that the frequency split nonlinear blending algorithm with fixed settings offered a superior differentiation of contrast levels from low- to high-contrast settings.

According to our results the combined use of all three imaging findings suggesting gangrenous cholecystitis increases sensitivity over the individual use of each of these signs. Nonetheless, rarely, frequency-selective non-linear blending can generate false-positive depending on the parameter setting, which can be further improved for future studies.

Of note, the interobserver agreement for frequency-selective non-linear blending -based reading was almost equal to that of linear blending-based reading suggesting minimal interreader variability for the novel post-processing technique.

Our study has some limitations. First, slightly different CECT protocols have been used in the diagnostic, but this would be expected to influence both reading techniques (linear blending and frequency-selective non-linear blending) equally. Second, there were some differences in the length of time of the interval between CECT and surgery, which possibly introduce the discrepancies between findings on CT and pathological examination. Third, some discrepancies between histology and CECT-reading might rely in the degree of gallbladder-wall ischemia which in incipient stages presumably eludes even detection by frequency-selective non-linear blending.

In conclusion, frequency-selective non-linear blending post-processing increases the diagnostic performance of CT for the diagnosis of gangrenous cholecystitis through more accurate detection of reduced or absent gallbladder-wall enhancement, ulcers, and perforation.

## Disclosure

Jan Fritz received institutional research support from Siemens Healthcare USA, DePuy, Zimmer, Microsoft, and BTG International; is a scientific advisor of Siemens Healthcare USA, Alexion Pharmaceuticals, and BTG International; received speaker's honorarium from Siemens Healthcare USA and has shared patents with Siemens Healthcare and Johns Hopkins University.

Marius Horger received institutional research support and speaker's honorarium from Siemens Healthcare Germany and GE Germany

## References

- W.-C. Chang, Y. Sun, E.-H. Wu, S.Y. Kim, Z.J. Wang, G.-S. Huang, B.M. Yeh, CT findings for detecting the presence of gangrenous ischemia in cholecystitis, *Am. J. Roentgenol.* 207 (2016) 302–309, <https://doi.org/10.2214/AJR.15.15658>.
- H. Maehira, M. Kawasaki, A. Itoh, M. Ogawa, N. Mizumura, S. Toyoda, S. Okumura, M. Kameyama, Prediction of difficult laparoscopic cholecystectomy for acute cholecystitis, *J. Surg. Res.* 216 (2017) 143–148, <https://doi.org/10.1016/j.jss.2017.05.008>.
- K.-H. Kim, S.-J. Kim, S.C. Lee, S.K. Lee, Risk assessment scales and predictors for simple versus severe cholecystitis in performing laparoscopic cholecystectomy, *Asian J. Surg.* 40 (2017) 367–374, <https://doi.org/10.1016/j.asjsur.2015.12.006>.
- R. Sinha, Difficult Laparoscopic Cholecystectomy-When and Where is the Need to Convert? *Apollo Med.* 7 (2010) 135–137, [https://doi.org/10.1016/S0976-0016\(11\)60095-1](https://doi.org/10.1016/S0976-0016(11)60095-1).
- M. Tomizawa, F. Shinozaki, S. Tanaka, T. Sunaoshi, D. Kano, E. Sugiyama, M. Shite, R. Haga, Y. Fukamizu, T. Fujita, S. Kagayama, R. Hasegawa, Y. Shirai, Y. Motoyoshi, T. Sugiyama, S. Yamamoto, N. Ishige, Diagnosis of complications associated with acute cholecystitis using computed tomography and diffusion-weighted imaging with background body signal suppression/T2 image fusion, *Exp. Ther. Med.* 14 (2017) 743–747, <https://doi.org/10.3892/etm.2017.4567>.
- A.K. Singh, P. Sagar, Gangrenous cholecystitis: prediction with CT imaging, *Abdom. Imaging* 30 (2005) 218–221, <https://doi.org/10.1007/s00261-004-0217-0>.
- M.-J. Tsai, J.-D. Chen, C.-M. Tiu, Y.-H. Chou, S.-C. Hu, C.-Y. Chang, Can acute cholecystitis with gallbladder perforation be detected preoperatively by computed tomography in ED? Correlation with clinical data and computed tomography features, *Am. J. Emerg. Med.* 27 (2009) 574–581, <https://doi.org/10.1016/j.ajem.2008.04.024>.
- D. Fuks, C. Mouly, B. Robert, H. Hajji, T. Yzet, J.-M. Regimbeau, Acute cholecystitis: preoperative CT can help the surgeon consider conversion from laparoscopic to open cholecystectomy, *Radiology* 263 (2012) 128–138, <https://doi.org/10.1148/radiol.12110460>.
- G.L. Bennett, H. Rusinek, V. Lisi, G.M. Israel, G.A. Krinsky, C.M. Slywotzky, A. Megibow, CT Findings in Acute Gangrenous Cholecystitis, *Am. J. Roentgenol.* 178 (2002) 275–281, <https://doi.org/10.2214/ajr.178.2.1780275>.
- C.-H. Wu, C.-C. Chen, C.-J. Wang, Y.-C. Wong, L.-J. Wang, C.-C. Huang, W.-C. Lo, H.-W. Chen, Discrimination of gangrenous from uncomplicated acute cholecystitis: accuracy of CT findings, *Abdom. Imaging* 36 (2011) 174–178, <https://doi.org/10.1007/s00261-010-9612-x>.
- N.B. Patel, A. Oto, S. Thomas, Multidetector CT of emergent biliary pathologic conditions, *Radiogr. Rev. Publ. Radiol. Soc. N. Am. Inc.* 33 (2013) 1867–1888, <https://doi.org/10.1148/rg.337125038>.
- P. Soyer, C. Hoeffel, A. Dohan, E. Gayat, C. Eveno, B. Malgras, K. Paurat, M. Boudiaf, Acute cholecystitis: quantitative and qualitative evaluation with 64-section helical CT, *Acta Radiol. Stockh. Swed.* 1987 54 (2013) 477–486, <https://doi.org/10.1177/0284185113475798>.
- H. Maehira, A. Itoh, M. Kawasaki, M. Ogawa, A. Imagawa, N. Mizumura, S. Okumura, M. Kameyama, Use of dynamic CT attenuation value for diagnosis of acute gangrenous cholecystitis, *Am. J. Emerg. Med.* 34 (2016) 2306–2309, <https://doi.org/10.1016/j.ajem.2016.08.033>.
- H. Derici, E. Kamer, C. Kara, H.R. Unalp, T. Tansug, A.D. Bozdog, O. Nazli, Gallbladder perforation: clinical presentation, predisposing factors, and surgical outcomes of 46 patients, *Turk. J. Gastroenterol.* 22 (2011) 505–512, <https://doi.org/10.4318/tjg.2011.0246>.
- S. Schneeweiss, M. Esser, W. Thaiss, H. Boesmueller, H. Ditt, K. Nikolaou, M. Horger, Improved CT-detection of acute bowel ischemia using frequency selective non-linear image blending, *Acta Radiol. Open* 6 (2017), <https://doi.org/10.1177/2058460117718224>.
- G. Bier, M.N. Bongers, H. Ditt, B. Bender, U. Ernemann, M. Horger, Enhanced gray-white matter differentiation on non-enhanced CT using a frequency selective non-linear blending, *Neuroradiology* 58 (2016) 649–655, <https://doi.org/10.1007/s00234-016-1674-1>.
- G. Bier, M.N. Bongers, H. Ditt, B. Bender, U. Ernemann, M. Horger, Accuracy of non-enhanced CT in detecting early ischemic edema using frequency selective non-linear blending, *PLoS One* 11 (2016) e0147378, <https://doi.org/10.1371/journal.pone.0147378>.
- M.N. Bongers, G. Bier, R. Marcus, H. Ditt, C. Kloth, C. Schabel, K. Nikolaou, M. Horger, Image quality of a novel frequency selective nonlinear blending algorithm: an ex vivo phantom study in comparison to single-energy acquisitions and dual-energy acquisitions with monoenergetic reconstructions, *Invest. Radiol.* 51 (2016) 647–654, <https://doi.org/10.1097/RLI.0000000000000293>.
- Y. Kimura, T. Takada, S.M. Strasberg, H.A. Pitt, D.J. Gouma, O.J. Garden, M.W. Buchler, J.A. Windsor, T. Mayumi, M. Yoshida, F. Miura, R. Higuchi, T. Gabata, J. Hata, H. Gomi, C. Dervenis, W.-Y. Lau, G. Belli, M.-H. Kim, S.C. Hilvano, Y. Yamashita, TG13 current terminology, etiology, and epidemiology of acute cholangitis and cholecystitis, *J. Hepato-Biliary-Pancreat. Sci.* 20 (n.d.) 8–23, doi:10.1007/s00534-012-0564-0.
- P.C. Ambe, H. Christ, D. Wassenberg, Does the Tokyo guidelines predict the extent of gallbladder inflammation in patients with acute cholecystitis? A single center retrospective analysis, *BMC Gastroenterol.* 15 (2015), <https://doi.org/10.1186/s12876-015-0365-4>.
- J. Rosai, *Rosai and Ackerman's Surgical Pathology E-Book*, Elsevier Health Sciences, 2011.
- Y. Yashima, T. Tsujino, S. Nakahara, K. Ishida, R. Nakata, H. Isayama, K. Koike, Contrast-enhanced ultrasonographic image of gangrenous gallbladder, *J. Med. Ultrason.* 38 (2011) 239, <https://doi.org/10.1007/s10396-011-0316-9>.
- I. Pedrosa, A. Guarise, J. Goldsmith, C. Procacci, N.M. Rofsky, The interrupted rim sign in acute cholecystitis: a method to identify the gangrenous form with MRI, *J. Magn. Reson. Imaging* 18 (2003) 360–363, <https://doi.org/10.1002/jmri.10356>.
- M.N. Bongers, G. Bier, C. Kloth, C. Schabel, J. Fritz, K. Nikolaou, M. Horger, Frequency selective non-linear blending to improve image quality in liver CT, *RöFo* 188 (2016) 1163–1168, <https://doi.org/10.1055/s-0042-116440> Georg Thieme Verlag KG Stuttgart, New York.
- R.A. Kruger, S.J. Riederer, C.A. Mistretta, Relative properties of tomography, K-edge imaging, and K-edge tomography, *Med. Phys.* 4 (1977) 244–249, <https://doi.org/10.1118/1.594374>.
- S.J. Riederer, C.A. Mistretta, Selective iodine imaging using K-edge energies in computerized x-ray tomography, *Med. Phys.* 4 (1977) 474–481, <https://doi.org/10.1118/1.594357>.